Cureus
Part of SPRINGER NATURE

Open Access Case Report

Diagnostic Challenges of Isolated Brainstem Tumefactive Demyelinating Lesion

Yuki Kamida [1, 2], Yosuke Takeuchi [1], Gekka Otsuka [1], Kaito Arimatsu [2], Yasutomo Momii [2], Nobuhiro Hata [2], Ryuichi Sato [3], Noriyuki Kimura [1]

1. Neurology, Faculty of Medicine, Oita University, Yufu, JPN 2. Neurosurgery, Faculty of Medicine, Oita University, Yufu, JPN 3. Neurology, Shin Beppu Hospital, Beppu, JPN

Corresponding author: Yosuke Takeuchi, ytakeuchi1225@oita-u.ac.jp

Review began 11/07/2026
Review ended 11/13/2026
Published 11/17/2026

© **Copyright** 2026
Kamida et al. This is an open access article distributed under the terms of the Creative Commons Attribution License CC-BY 4.0., which permits unrestricted use, distribution, and reproduction in any medium, provided the original author and source are credited.

DOI: 10.7759/cureus.119804

Abstract

Tumefactive demyelinating lesion (TDL) is a variant of inflammatory demyelinating disease that mimics brain tumors. Brainstem TDL is particularly difficult to distinguish from neoplasms because histopathological confirmation is often challenging. We herein present a case of isolated brainstem TDL that was initially suspected to represent a brain tumor. Although a brain biopsy could not be performed, open-ring enhancement and increased apparent diffusion coefficient values on MRI, together with CSF findings suggestive of inflammation rather than neoplasia, supported the clinical diagnosis of TDL. This case highlights the diagnostic challenges of isolated brainstem TDL.

Categories: Neurology, Internal Medicine, Neurosurgery
Keywords: apparent diffusion coefficient, brainstem, liquid biopsy, open-ring enhancement, tumefactive demyelinating lesion

Introduction

Tumefactive demyelinating lesion (TDL) is an uncommon variant of inflammatory demyelinating disease characterized by a tumor-like appearance, typically presenting as a lesion measuring >2 cm in diameter with mass effect, perilesional edema, and contrast enhancement [1]. The clinical and radiological features of TDL closely mimic those of brain tumors, and differentiating between the two conditions is often challenging [2]. Because TDL usually responds favorably to immunotherapy [3], misdiagnosis may lead to unnecessary invasive procedures or inappropriate treatment.

TDL predominantly appears in supratentorial white matter, whereas isolated brainstem involvement is rare [4,5]. Because of this unusual distribution and tumor-like appearance, brainstem TDL may be difficult to recognize and can be mistaken for neoplasms, such as glioma and primary central nervous system lymphoma (PCNSL). Furthermore, brainstem lesions produce diverse neurological manifestations, including cranial nerve palsies, motor weakness, sensory disturbances, and ataxia [6], and delayed treatment may result in irreversible neurological deficits. Early diagnosis and initiation of appropriate therapy are therefore crucial.

We herein report a case of isolated brainstem TDL that posed a diagnostic challenge because histopathological confirmation by brain biopsy was difficult.

Case Presentation

A 58-year-old woman was admitted to a local general hospital with gait disturbance that had started two months earlier. She also developed hoarseness, dysphagia, and numbness on the right side of the body, including the face, one month after symptom onset. Brain MRI showed a tumor-like lesion on the left side of the brainstem, and she was transferred to the Department of Neurosurgery at our hospital on day 4 of hospitalization. The differential diagnosis included neoplasms, inflammatory demyelinating diseases, and neurosarcoidosis; however, brain biopsy was considered to carry a high risk of neurological complications, making histopathological confirmation difficult. The patient was transferred to our department for further evaluation on day 18 of hospitalization. Neurological examination revealed left Horner syndrome, left abducens nerve palsy, horizontal gaze-evoked nystagmus, decreased sensation to touch, temperature, and pain on the right side of the body, including the face, left peripheral facial palsy, left sensorineural hearing loss, dysarthria, hoarseness, hypernasal speech, dysphagia, right-predominant quadriparesis (muscle strength graded as 3-4 in the right upper and lower extremities and 4-5 in the left upper and lower extremities on manual muscle testing), and limb and truncal ataxia. She was bedridden and required tube feeding.

The laboratory and CSF findings are shown in Table *1*. Blood tests showed elevated IgA (429 mg/dL) and soluble interleukin-2 receptor (sIL-2R) levels (768 U/mL). An IgG-κ monoclonal protein was detected. Anti-aquaporin-4 and anti-myelin oligodendrocyte glycoprotein (MOG) antibodies (cell-based assay) were negative. CSF examination revealed pleocytosis (99 cells/μL, 100% mononuclear cells), an elevated IgG

How to cite this article
Kamida Y, Takeuchi Y, Otsuka G, et al. (November 17, 2026) Diagnostic Challenges of Isolated Brainstem Tumefactive Demyelinating Lesion. Cureus 18(11): e119804. DOI 10.7759/cureus.119804

index (1.04), and elevated myelin basic protein levels (255.0 pg/mL). CSF protein, sIL-2R, and IL-10 levels were normal. Five oligoclonal bands were detected. Anti-MOG antibody (cell-based assay) testing was negative. The FilmArray Meningitis/Encephalitis Panel (bioMérieux, Marcy-l'Étoile, France) and PCR testing for *Mycobacterium tuberculosis* were negative. Cytology revealed atypical cells, but the findings were not diagnostic of malignancy. The MYD88 L265P, IDH1, H3K27M, BRAF, and TERT promoter mutations were not detected in CSF.

Variable	Value	Reference range	Variable	Value	Reference range
Blood tests			CSF tests		
White blood cell count	8,250/μL	3,300-8,600/μL	Cell count (mononuclear cells)	99/μL (100%)	0-5/μL
Hemoglobin	15.1 g/dL	11.6-14.8 g/dL	Protein	38.4 mg/dL	10.0-45.0 mg/dL
Platelet count	443 × 10^3/μL	158-348 × 10^3/μL	sIL-2R	<50 U/mL	<50 U/mL
Total protein	6.8 g/dL	6.6-8.1 g/dL	IL-10	<0.78 pg/mL	<0.78 pg/mL
Albumin	3.2 g/dL	4.1-5.1 g/dL	IgG index	1.04	<0.70
Sodium	139.0 mEq/L	138.0-145.0 mEq/L	Myelin basic protein	255.0 pg/mL	<102.0 pg/mL
Potassium	3.8 mEq/L	3.6-4.8 mEq/L	Oligoclonal bands	5 bands	Negative
Chloride	100.7 mEq/L	101.0-108.0 mEq/L	Anti-MOG antibody (CBA)	Negative	Negative
Total bilirubin	0.4 mg/dL	0.4-1.5 mg/dL	*Mycobacterium tuberculosis* PCR	Negative	Negative
AST	24.0 U/L	13.0-30.0 U/L	FilmArray ME Panel	Negative	Negative
ALT	22.6 U/L	7.0-23.0 U/L	Cytology	Atypical cells	-
LDH	214 U/L	124-222 U/L	Liquid biopsy		
γ-GTP	28.6 U/L	9.0-32.0 U/L	MYD88 L265P mutation	Negative	Negative
BUN	16.7 mg/dL	8.0-20.0 mg/dL	IDH1 mutation	Negative	Negative
Creatinine	0.61 mg/dL	0.46-0.79 mg/dL	H3K27M mutation	Negative	Negative
CRP	0.91 mg/dL	0.00-0.14 mg/dL	BRAF mutation	Negative	Negative
IgG	1,050 mg/dL	861-1,747 mg/dL	TERT promoter mutation	Negative	Negative
IgA	429 mg/dL	93-393 mg/dL	-	-	-
IgM	123 mg/dL	50-269 mg/dL	-	-	-
sIL-2R	768 U/mL	122-496 U/mL	-	-	-
Monoclonal protein	IgG-κ	Negative	-	-	-
Anti-AQP4 antibody (CBA)	Negative	Negative	-	-	-
Anti-MOG antibody (CBA)	Negative	Negative	-	-	-

TABLE 1: Laboratory and CSF findings.

ALT, alanine aminotransferase; AQP4, aquaporin-4; AST, aspartate aminotransferase; BUN, blood urea nitrogen; CBA, cell-based assay; γ-GTP, gamma-glutamyl transferase; IDH1, isocitrate dehydrogenase 1; LDH, lactate dehydrogenase; ME, meningitis/encephalitis; MOG, myelin oligodendrocyte glycoprotein; sIL-2R, soluble interleukin-2 receptor; TERT, telomerase reverse transcriptase

Bone marrow biopsy showed no evidence of neoplastic plasma cell proliferation. Whole-body 18F-fluorodeoxyglucose PET revealed no abnormal uptake indicative of malignancy. Brain MRI demonstrated hyperintense lesions on the left side of the medulla oblongata and in the left dorsal pons on diffusion-weighted imaging (Figure *1A*, *1D*), with increased apparent diffusion coefficient (ADC) values (Figure *1B*, *1E*) and hyperintensity on fluid-attenuated inversion recovery imaging (Figure *1C*, *1F*). Both lesions exhibited open-ring enhancement (Figure *2A*, *2B*). The brainstem lesion measured >2 cm in its maximal craniocaudal dimension (Figure *2C*).

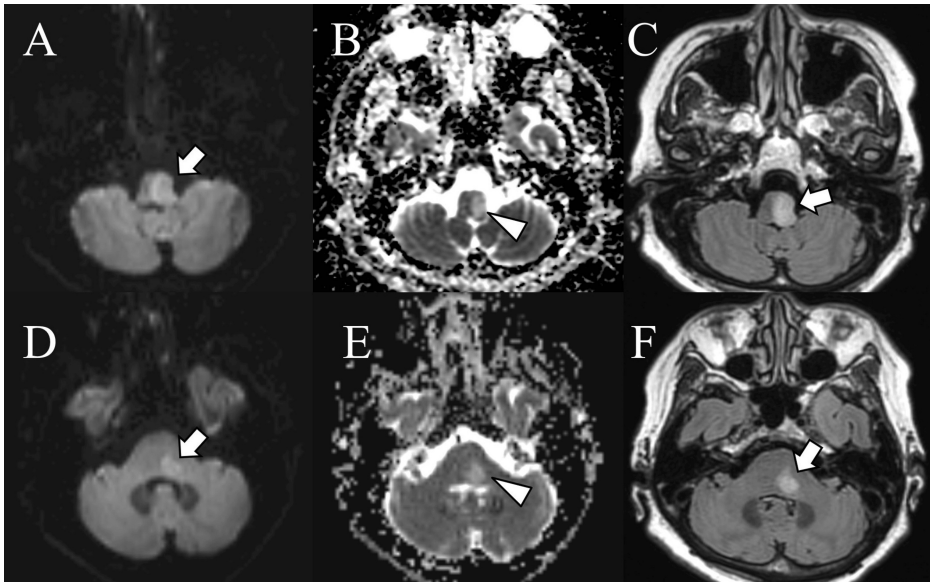


FIGURE 1: Brain MRI on admission.

Brain MRI revealed hyperintense lesions on the left side of the medulla oblongata and in the left dorsal pons on diffusion-weighted imaging (A and D, arrows), with increased ADC values (B and E, arrowheads) and hyperintensity on fluid-attenuated inversion recovery imaging (C and F, arrows).

ADC, apparent diffusion coefficient

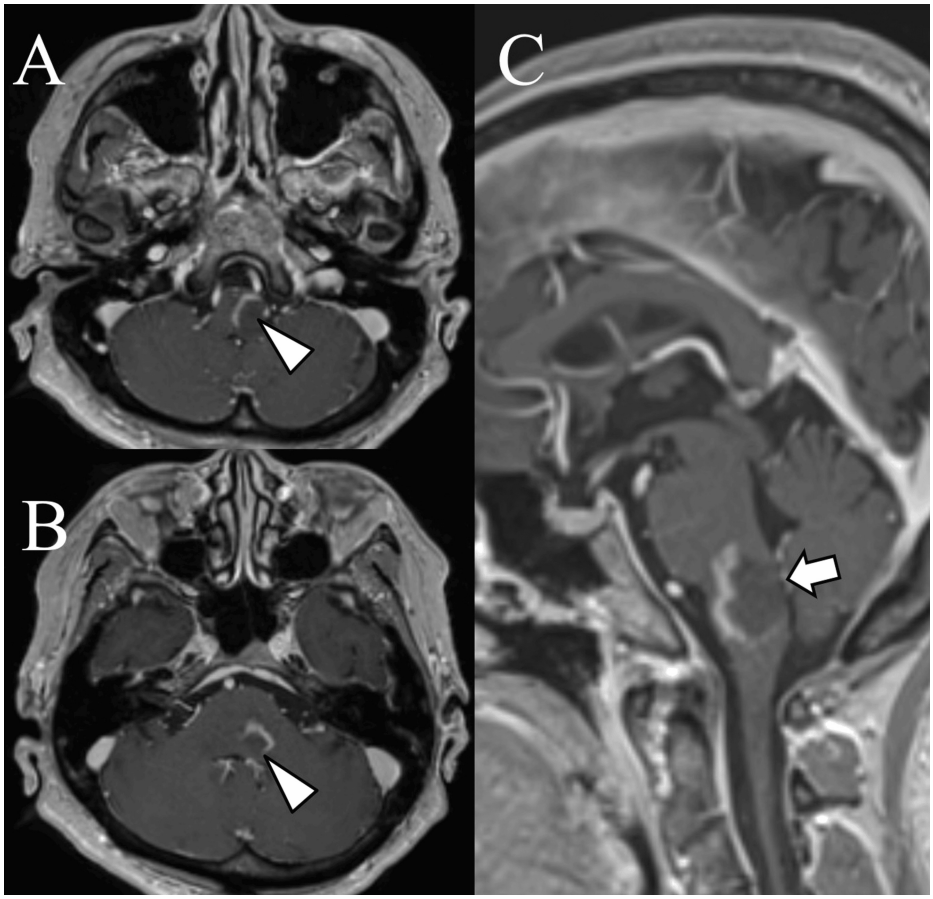


FIGURE 2: Contrast-enhanced brain MRI on admission.

Contrast-enhanced brain MRI revealed open-ring enhancement of lesions on the left side of the medulla oblongata and in the left dorsal pons (A and B, arrowheads). The brainstem lesion measured >2 cm in its maximal craniocaudal dimension (C, arrow).

The central vein sign and paramagnetic rim lesions, which are characteristic MRI features of multiple sclerosis, were not observed on T2*-weighted gradient-echo imaging. Magnetic resonance spectroscopy (MRS) revealed elevated choline and lactate peaks with preserved N-acetylaspartate. Reliable perfusion assessment using arterial spin labeling (ASL) was difficult because of the small lesion size. Magnetic resonance angiography revealed no stenosis of the vertebral or basilar arteries. Spinal MRI revealed no lesions.

The patient was clinically diagnosed with isolated TDL and was treated with two courses of steroid pulse therapy (methylprednisolone, 1,000 mg/day for five days in the first course and three days in the second course), followed by oral prednisolone (55 mg/day). The neurological symptoms markedly improved, and she regained the ability to eat orally and walk independently. Brain MRI on day 65 of hospitalization revealed a reduction in the size of the brainstem lesions (Figure *3A*-*3F*). After prednisolone was gradually tapered by 10 mg every two weeks, she was transferred for rehabilitation on day 67 of hospitalization.

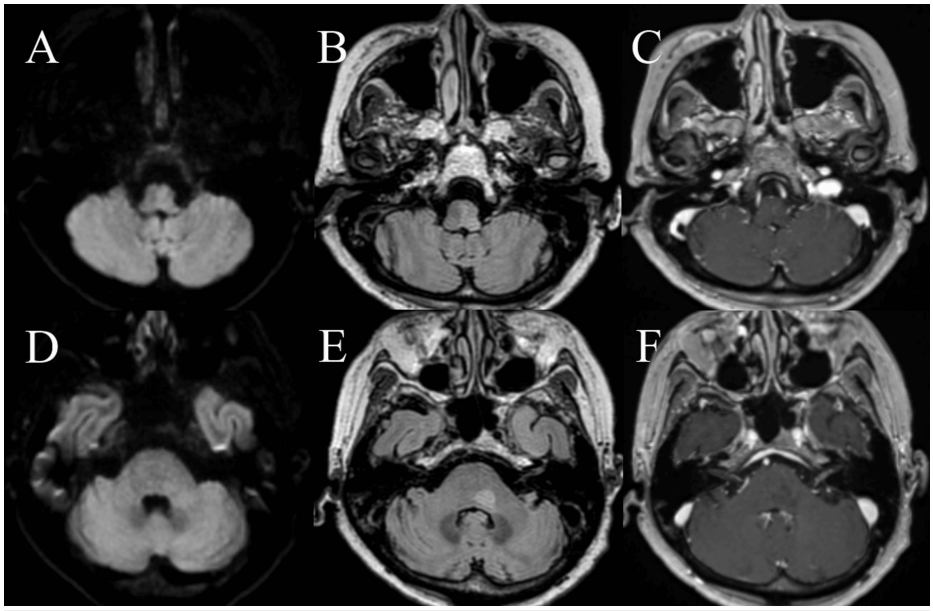


FIGURE 3: Brain MRI after treatment.

After immunotherapy, the hyperintense lesions in the pons and medulla oblongata decreased in size on diffusion-weighted imaging (A and D) and fluid-attenuated inversion recovery imaging (B and E), and the open-ring enhancement of both lesions disappeared (C and F).

Discussion

We herein describe a case of TDL confined to the brainstem that presented with diverse neurological manifestations and was initially suspected to represent a brain tumor because of its mass effect. Because brain biopsy was difficult owing to the anatomical location of the lesion, differentiation from neoplasms was challenging. MRI findings, including open-ring enhancement and increased ADC values, favored TDL over a brain tumor, while CSF investigations further supported an inflammatory demyelinating disorder. These findings led to a clinical diagnosis of TDL despite the lack of histopathological confirmation.

Although TDL mainly occurs in supratentorial white matter, brainstem lesions have also been reported [4,5]. Differentiating TDL from brain tumors, particularly glioma and PCNSL, is challenging, and histopathological confirmation is often required for diagnosis [2]. This presents a clinical dilemma because biopsy of brainstem lesions may carry a substantial risk of severe neurological complications. How can isolated brainstem TDL be diagnosed without brain biopsy? Characteristic MRI findings provide important diagnostic clues. Open-ring enhancement has been reported in 35% of TDLs and has a specificity of 98% for differentiating TDL from brain tumors [1], and ADC values are significantly higher in TDL than in glioma or PCNSL and may also aid differentiation [7]. Although these findings are well recognized in TDL, their diagnostic value may be particularly high in uncommon brainstem presentations, in which brain biopsy is considered high risk, as in our case. Although MRS may be useful in differentiating TDL from brain tumors and abscesses [8,9], elevated choline and lactate peaks with preserved N-acetylaspartate, as in our case, are not specific to TDL. Similarly, ASL can help distinguish TDL from high-grade gliomas, which generally exhibit higher cerebral blood flow [10], although ASL assessment was limited by the small lesion size in the present case.

CSF investigations may also aid in differentiating inflammatory demyelination from neoplasms. In the present case, an elevated IgG index, oligoclonal bands, and increased myelin basic protein levels supported an inflammatory demyelinating process. In addition, CSF-based liquid biopsy testing for the MYD88 L265P, IDH1, H3K27M, BRAF, and TERT promoter mutations was performed to evaluate potential neoplastic conditions; none of these mutations was detected. The MYD88 L265P mutation in CSF is highly specific for PCNSL [11], whereas IDH1, H3K27M, BRAF, and TERT promoter mutations can be detected in CSF-derived tumor DNA from patients with diffuse glioma [12,13]. The reported sensitivities and specificities of CSF-based detection were 92.2-100% and 100% for MYD88 L265P [11], 84.6% and 100% for H3K27M, and 80.0% and 100% for BRAF V600E mutations, respectively [13]. Although negative liquid biopsy results cannot definitively exclude neoplasms [14], these findings provide complementary information when evaluating neoplastic mimics of TDL. The combination of characteristic MRI findings and inflammatory CSF abnormalities, supplemented by molecular testing for neoplasms, may facilitate clinical diagnostic decision-making in patients with suspected brainstem TDL.

A limitation of this case report is the lack of histopathological confirmation and the limited duration of MRI

follow-up; therefore, brain tumors, particularly PCNSL, could not be completely excluded. However, the characteristic MRI findings, normal CSF IL-10 level, absence of the MYD88 L265P mutation and other tumor-associated genetic alterations in CSF, and favorable response to immunotherapy collectively supported the clinical diagnosis of TDL.

Conclusions

We described a case of isolated brainstem TDL that was initially suspected to represent a brain tumor. This case highlights the diagnostic challenges of TDL when brain biopsy is not feasible. In this setting, although histopathological confirmation is unavailable, characteristic MRI findings, including open-ring enhancement and increased ADC values, and complementary CSF investigations may support the clinical diagnosis of TDL and guide treatment decisions.

Additional Information

Author Contributions

All authors have reviewed the final version to be published and agreed to be accountable for all aspects of the work.

Concept and design: Yosuke Takeuchi, Yuki Kamida

Acquisition, analysis, or interpretation of data: Yosuke Takeuchi, Noriyuki Kimura, Ryuichi Sato, Gekka Otsuka, Yuki Kamida, Kaito Arimatsu, Yasutomo Momii, Nobuhiro Hata

Drafting of the manuscript: Yosuke Takeuchi, Yuki Kamida

Critical review of the manuscript for important intellectual content: Yosuke Takeuchi, Noriyuki Kimura, Ryuichi Sato, Gekka Otsuka, Yuki Kamida, Kaito Arimatsu, Yasutomo Momii, Nobuhiro Hata

Supervision: Noriyuki Kimura, Nobuhiro Hata

Disclosures

Human subjects: Informed consent for treatment and open access publication was obtained or waived by all participants in this study. **Conflicts of interest:** In compliance with the ICMJE uniform disclosure form, all authors declare the following: **Payment/services info:** All authors have declared that no financial support was received from any organization for the submitted work. **Financial relationships:** All authors have declared that they have no financial relationships at present or within the previous three years with any organizations that might have an interest in the submitted work. **Other relationships:** All authors have declared that there are no other relationships or activities that could appear to have influenced the submitted work.

Acknowledgements

Yuki Kamida and Yosuke Takeuchi contributed equally to this work. We would like to thank all members of the Department of Neurology and Neurosurgery, Oita University Hospital, for helping with the collection of clinical data. We acknowledge the use of ChatGPT (OpenAI, Inc., San Francisco, CA, USA) to assist with English-language editing and improve manuscript readability.

References

1. Suh CH, Kim HS, Jung SC, Choi CG, Kim SJ: MRI findings in tumefactive demyelinating lesions: a systematic review and meta-analysis. AJNR Am J Neuroradiol. 2018, 39:1643-9. 10.3174/ajnr.A5775
2. Hardy TA, Chataway J: Tumefactive demyelination: an approach to diagnosis and management. J Neurol Neurosurg Psychiatry. 2013, 84:1047-53. 10.1136/jnnp-2012-304498
3. Vakrakou AG, Tzanetakos D, Evangelopoulos ME, et al.: Clinico-radiologic features and therapeutic strategies in tumefactive demyelination: a retrospective analysis of 50 consecutive cases. Ther Adv Neurol Disord. 2021, 14:17562864211006503. 10.1177/17562864211006503
4. Al Malik YM: Tumefactive demyelinating lesions: a literature review of recent findings . Neurosciences (Riyadh). 2024, 29:153-60. 10.17712/nsj.2024.3.20230111
5. Mitsutake A, Sato T, Katsumata J, et al.: Tumefactive multiple sclerosis which initially presented with brainstem encephalitis with a long-term follow-up. Mult Scler Relat Disord. 2019, 32:23-6. 10.1016/j.msard.2019.04.018
6. Benghanem S, Mazeraud A, Azabou E, et al.: Brainstem dysfunction in critically ill patients . Crit Care. 2020, 24:5. 10.1186/s13054-019-2718-9
7. Mabray MC, Cohen BA, Villanueva-Meyer JE, Valles FE, Barajas RF, Rubenstein JL, Cha S: Performance of apparent diffusion coefficient values and conventional MRI features in differentiating tumefactive demyelinating lesions from primary brain neoplasms. AJR Am J Roentgenol. 2015, 205:1075-85. 10.2214/AJR.14.13970
8. Saindane AM, Cha S, Law M, et al.: Proton MR spectroscopy of tumefactive demyelinating lesions . AJNR Am

J Neuroradiol. 2002, 23:1378-86.
9. Kadota O, Kohno K, Ohue S, Kumon Y, Sakaki S, Kikuchi K, Miki H: Discrimination of brain abscess and cystic tumor by in vivo proton magnetic resonance spectroscopy. Neurol Med Chir (Tokyo). 2001, 41:121-6. 10.2176/nmc.41.121
10. Soni N, Srindharan K, Kumar S, Mishra P, Bathla G, Kalita J, Behari S: Arterial spin labeling perfusion: prospective MR imaging in differentiating neoplastic from non-neoplastic intra-axial brain lesions. Neuroradiol J. 2018, 31:544-53. 10.1177/1971400918783058
11. Yamagishi Y, Sasaki N, Nakano Y, et al.: Liquid biopsy of cerebrospinal fluid for MYD88 L265P mutation is useful for diagnosis of central nervous system lymphoma. Cancer Sci. 2021, 112:4702-10. 10.1111/cas.15133
12. Fujioka Y, Hata N, Akagi Y, et al.: Molecular diagnosis of diffuse glioma using a chip-based digital PCR system to analyze IDH, TERT, and H3 mutations in the cerebrospinal fluid. J Neurooncol. 2021, 152:47-54. 10.1007/s11060-020-03682-7
13. Madlener S, Stepien N, Senfter D, et al.: Detection of H3F3A K27M or BRAF V600E in liquid biopsies of brain tumor patients as diagnostic and monitoring biomarker: impact of tumor localization and sampling method. Acta Neuropathol. 2025, 149:5. 10.1007/s00401-024-02842-7
14. Bale TA, Mellinghoff IK, Graham MS: Liquid biopsy in the diagnosis of primary brain tumors . Adv Cancer Res. 2025, 166:81-102. 10.1016/bs.acr.2025.05.004